

IMpack: open source high-bandwidth data-logging inertial measurement unit

John T. Antolik¹ and Daniel M. Harris^{1*}

¹*Brown University, School of Engineering, 184 Hope St., Providence RI 02912*
**Correspondence email address: daniel_harris3@brown.edu*

March 12, 2025

Abstract

IMpack is a single-board data-logging inertial measurement unit (IMU) designed for research applications where sampling rate, compactness, and cost effectiveness are paramount. The battery-powered device features an array of micro-electromechanical system (MEMS) accelerometer chips which allow it to achieve a maximum acceleration measurement range of ± 400 g, sampling rates up to 26.6 kHz, and an angular rate measurement range of ± 2000 deg/s. In this article we describe the hardware and software design of the device and present frequency response measurements using a shaker setup that validate the high-bandwidth performance of the IMpack. We demonstrate a research use case in which we embed the IMpack in an aluminum structure and measure the force of impact as the structure lands on the water surface, showing that the result compares favorably against an industry standard commercial IMU. This accessible low-cost IMU platform will enable highly resolved acceleration measurements in a range of engineering research and design areas, as well as in educational settings.

Metadata Overview

Main design files: <https://github.com/harrislab-brown/IMpack>

Target group: engineering research and design, engineering education.

Skills required: PCB manufacturing - specialist; surface mount soldering - advanced; 3D printing - easy; CNC machining - advanced.

Replication: 20 units have been constructed by the authors, including 10 of the final version whose performance is reported herein and are actively used for water entry research experiments within our group.

Keywords

inertial measurement unit; IMU; accelerometer; gyroscope; vibration; modal analysis; impact; laboratory; data logging; frequency response; mechanical engineering

(1) Overview

Introduction

Highly resolved acceleration measurements are vital in a range of engineering application areas including robotics, biomedical devices, navigation, and manufacturing (Ahmad et al. 2013). In many situations, battery-powered inertial measurement units (IMUs) with integrated data logging are necessary to measure dynamics of an untethered body in motion, ideally using a compact sensor with low mass so the presence of the IMU exerts minimal dynamic influence on the system. In engineering research, such IMUs are used in areas like water surface impacts (Antolik et al. 2023) or animal flight (Friman et al. 2024). These areas of study and many others feature fast dynamics requiring high-bandwidth acceleration sensing. As of the time of writing this article, commercial options that exceed 1 kHz sampling rate typically cost at least several hundred USD. Options are limited for sample rates that exceed 10 kHz and costs increase accordingly, to values often in the several thousand USD (Hanly 2019). Some authors resort to bespoke DIY solutions (Debenedetti & Jung 2024, Rabbi et al. 2021), motivating the need for an open source reference design for a data-logging IMU. Here we present the IMpack, a highly compact single board data-logging IMU with sample rates up to 26.6 kHz that can be fabricated for less than 100 USD. In this article we describe its design and usage, validate its performance against reference accelerometers in a shaker test setup, and demonstrate its application to the water impact research area.

Overall Implementation and design

The IMpack is designed as a single printed circuit board (PCB) for simplicity and compactness, with connectors and switches accessible to the user on the top side of the board and the IMU chips and battery charging circuit on the

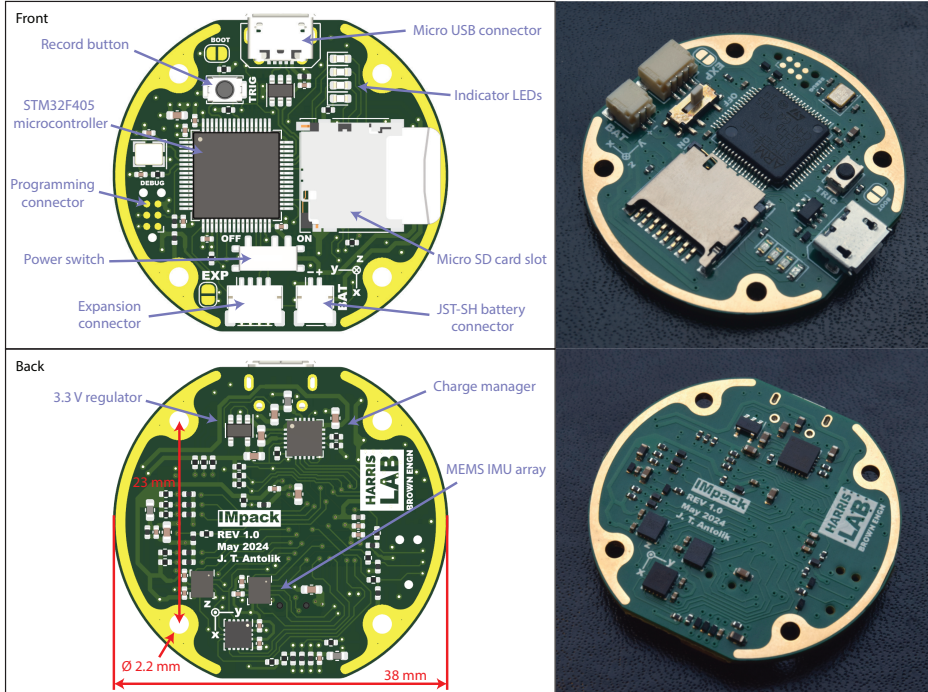


Figure 1: Renderings of the front and back of the IMpack (left) with the major components labeled, including overall dimensions of the board and the mounting hole pattern. Photographs of the front and back of the assembled IMpack PCB are also shown (right). The overall diameter of the IMpack is 38 mm and it can be mounted to a fixture using four M2 or #2 screws in a square pattern with 23 mm side length. The overall thickness including the battery is 13 mm. The mass of the IMpack PCB alone is 5 grams, and the mass including the battery is 9 grams.

Sensor	Sample rate (kHz)	Bandwidth (kHz)	Range	Bit depth
IIS3DWB	26.6	6.3	± 16 g	16
LSM6DSO32 (accel.)	6.66	3.33	± 32 g	16
LSM6DSO32 (gyro.)	6.66	1.44	± 2000 deg/s	16
ADXL373	5.12	2.56	± 400 g	12

Table 1: Specifications of the IMU chip sensors used in the IMpack design. Each channel can measure in three axes.

bottom side of the board as shown in figure 1. The IMpack is based around the STM32F405 microcontroller unit (MCU) which reads and logs data from three digital micro-electromechanical system (MEMS) IMU chips via the Serial Peripheral Interface (SPI). The MCU is programmed and debugged using an STLink debugger with a Tag-Connect TC2030 header. Accelerometer and gyroscope data are recorded to a micro SD card in a slot on the front side of the board. User interactions with the device occur via the main power switch and the recording button, with four light emitting diodes (LEDs) in different colors to indicate the state of the device. The IMpack can be powered either from a USB connection or from a single cell lithium polymer (LiPo) battery that connects to the battery connector (2-pin JST-SH). The charge managing/power multiplexing circuitry is assembled on the rear of the board, allowing the battery to be conveniently recharged from a USB power source. Finally, an expansion connector based on the STEMMA QT pinout is provided with access to the MCU general purpose input/output (GPIO) pins or Inter-Integrated Circuit (I2C) communication peripheral in order to allow future expansion to the IMpack functionality by providing the hardware for it to communicate with other devices. The IMpack PCB uses four copper layers to facilitate routing in the confined space. The two inner layers are ground planes for improved signal integrity and the signals and power are routed on the outer layers. The overall diameter of the IMpack is 38 mm and it can be mounted to a fixture using four M2 or #2 screws in a square pattern with 23 mm side length. The overall thickness including the battery is 13 mm. The mass of the IMpack PCB alone is 5 grams, and the total mass with the 150 mAh battery (TinyCircuits ASR00003) is 9 grams.

The MEMS IMU parts used and their primary specifications are listed in table 1. All of the chips measure acceleration in three axes and the LSM6DSO32 additionally contains a gyroscope. Sensor components with different strengths are chosen to improve the versatility of the device in different measurement situations. For instance, the IIS3DWB provides a very high sampling rate of 26.6 kHz but a small measurement range of ± 16 g. On the other hand, the ADXL373 provides a very large measurement range of ± 400 g but a smaller sampling rate of 5.12 kHz. Since all of the chips communicate digitally over the SPI interface, an IMU chip model could be swapped without influencing the rest of the design, allowing the IMpack to evolve as new IMU chips come to market or should the user identify another chip more appropriate to their application. When performing a recording, the IMpack can be configured to gather data from any subset of the IMU chips, including from all of them at maximum sampling rate. Several of the sensors have adjustable sampling rate, filter bandwidth, and measurement range which can be configured in the IMpack settings file. The IMpack firmware uses an interrupt based scheme to retrieve data from the

IMU chips resulting in minimum latency in which the MCU listens to the data-ready pin from each chip and initiates the SPI data read on the appropriate edges of the data-ready pin signal. The SPI read subroutine uses direct register manipulation for improved speed. Each data packet is tagged with a time stamp and an identifier for which chip of origin, and inserted into a large double buffer in random access memory (RAM). The buffer is written to a file on the SD card in binary format periodically as each half of the buffer is filled. Finally, at the end of the recording, the binary data file is read back and converted into a comma-separated value (CSV) text file with labeled columns on the SD card for more convenient processing by the user.

The flow of operation of the IMpack is illustrated in figure 2. The battery may be charged with the power switch in either the on or off position, with the red, orange, and green LEDs indicating the power and charge status. When the IMpack is first powered on, it will perform checks on the sensors and SD card. If the checks pass, it will set up the recording parameters based on the settings file (“settings.txt”) on the SD card, whose entries are described in table 2. If a valid settings file is found and the parameters are successfully configured, the blue LED will blink twice during the setup phase. If the settings file is absent or contains syntax errors, the blue LED will blink four times during the setup phase. In this case the IMpack will fall back to default parameters and a default settings file (annotated example in the associated documentation) will be created on the SD card. This is the recommended procedure to generate the initial configuration for the IMpack. The settings file can subsequently be edited to configure the aforementioned IMU chip sampling parameters as well as the parameters for starting and stopping the recording, including capabilities to perform a delayed start or triggering based on the acceleration level. When using the IMpack, a recording can be initiated by pressing the record button and will stop after either the configured recording time, or upon another press of the button. Once the IMpack returns to the idle state, it can be powered off and the SD card removed to extract the recorded data or adjust the settings.

(2) Quality control

Calibration

The IMpack acceleration measurements are compared to a reference accelerometer at a range of frequencies using the shaker test setup shown in figure 3(A). An aluminum fixture for the IMpack was designed that attaches to a modal shaker (Modal Shop K2007E01) as shown in figure 3(B), allowing the IMpack to be accelerated vertically with adjustable frequency and amplitude. The fixture was designed using modal analysis simulation software so that its free natural frequency is 11 kHz, exceeding the frequency range of our experimental testing. Two uniaxial reference accelerometers (PCB Piezotronics 352C65) thread into the bottom of the fixture at the front and back; the difference between their acceleration readings can be used as a proxy for the off-axis vibration in the shaker system (Harris & Bush 2015). The reference accelerometer calibration test reports indicate less than 2.5% measurement amplitude error from 0.5 Hz to 10 kHz. The accelerometers plug into a signal conditioner (PCB Piezotronics 482C05) and the measurement is subsequently captured by a dig-

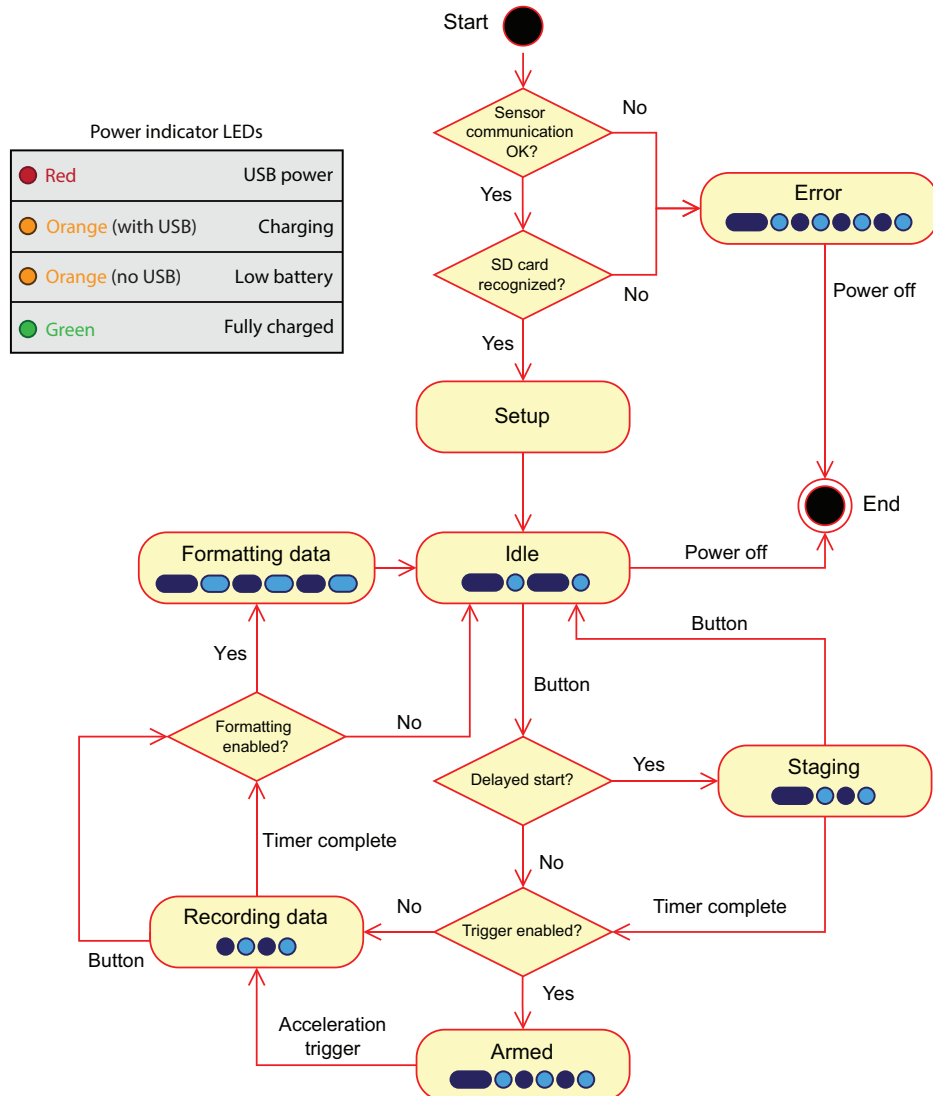


Figure 2: Flow chart diagram of the operation sequence of the IMpack. Based on the configured settings a recording can start immediately when the button is pressed, with some time delay or in response to an acceleration trigger event. The blink sequence of the blue indicator LED while in each state is illustrated in the diagram, where the width of each marker indicates the duration of the blink and the color indicates on or off. The power indicator LED table above lists the meanings of the other indicator LEDs.

Setting	Description	Allowed values
LSM6DSx_accel_enabled	Enables the LSM6DSx accelerometer	0 or 1
LSM6DSx_accel_odr_hz	Sample rate of the LSM6DSx accelerometer in Hz	13, 26, 52, 104, 208, 416, 833, 1660, 3330, or 6660
LSM6DSx_accel_range_g	Measurement range of the LSM6DSx accelerometer in g	4, 8, 16, or 32
LSM6DSx_accel_lpf	Low pass filter of the LSM6DSx accelerometer; a value of 2 sets the filter corner frequency to half the sampling frequency and so on	2, 4, 10, 20, 45, 100, 200, 400, or 800
LSM6DSx_accel_offset_x_mg	DC offset of the LSM6DSx accelerometer x axis in milli-g	signed integer
LSM6DSx_accel_offset_y_mg	DC offset of the LSM6DSx accelerometer y axis in milli-g	signed integer
LSM6DSx_accel_offset_z_mg	DC offset of the LSM6DSx accelerometer z axis in milli-g	signed integer
LSM6DSx_gyro_enabled	Enables the LSM6DSx gyroscope	0 or 1
LSM6DSx_gyro_odr_hz	Sample rate of the LSM6DSx gyroscope in Hz	13, 26, 52, 104, 208, 416, 833, 1660, 3330, or 6660
LSM6DSx_gyro_range_dps	Measurement range of the LSM6DSx gyroscope in deg/s	125, 250, 500, 1000, or 2000
LSM6DSx_gyro_lpf	Low pass filter of the LSM6DSx gyroscope; consult table 60 in LSM6DSO32 data sheet for interpretation	0, 1, 2, 3, 4, 5, 6, or 7
IIS3DWB_accel_enabled	Enables the IIS3DWB accelerometer	0 or 1
IIS3DWB_accel_range_g	Measurement range of the IIS3DWB accelerometer in g	2, 4, 8, 16
IIS3DWB_accel_lpf	Low pass filter of the IIS3DWB; a value of 4 sets the filter corner frequency to a quarter of the sampling frequency and so on	4, 10, 20, 45, 100, 200, 400, 800
IIS3DWB_accel_offset_x_mg	DC offset of the IIS3DWB accelerometer x axis in milli-g	signed integer
IIS3DWB_accel_offset_y_mg	DC offset of the IIS3DWB accelerometer y axis in milli-g	signed integer
IIS3DWB_accel_offset_z_mg	DC offset of the IIS3DWB accelerometer z axis in milli-g	signed integer
ADXL37x_accel_enabled	Enables the ADXL37x accelerometer	0 or 1
ADXL37x_accel_odr_hz	Sample rate of the ADXL37x accelerometer in Hz	320, 640, 1280, 2560, 5120
ADXL37x_accel_lpf	Low pass filter of the ADXL37x accelerometer; a value of 2 sets the filter corner frequency to half the sampling frequency and so on	2, 4, 8, 16, 32
ADXL37x_accel_offset_x_mg	DC offset of the ADXL37x accelerometer x axis in milli-g	signed integer
ADXL37x_accel_offset_y_mg	DC offset of the ADXL37x accelerometer y axis in milli-g	signed integer
ADXL37x_accel_offset_z_mg	DC offset of the ADXL37x accelerometer z axis in milli-g	signed integer
delay_before_armed_ms	Time in ms to remain in the staging state before recording	unsigned integer
recording_length_ms	Length of the recording in ms	unsigned integer
data_formatting_enabled	If enabled, generates plain text CSV files of recorded data	0 or 1
accel_trigger_enabled	Enables or disables acceleration triggering	0 or 1
accel_trigger_on_any_axis	If enabled, looks for the trigger threshold acceleration on any axis	0 or 1
accel_trigger_axis	If not triggering on any axis, this selects which axis to use for the trigger	0, 1, or 2 (x, y, or z)
accel_trigger_level_mg	Level of the acceleration trigger in milli-g	signed integer
accel_trigger_rising_edge	If enabled, triggers when acceleration magnitude exceeds the threshold, else when it falls below the threshold	0 or 1

Table 2: Description of the elements in the IMpack settings file.

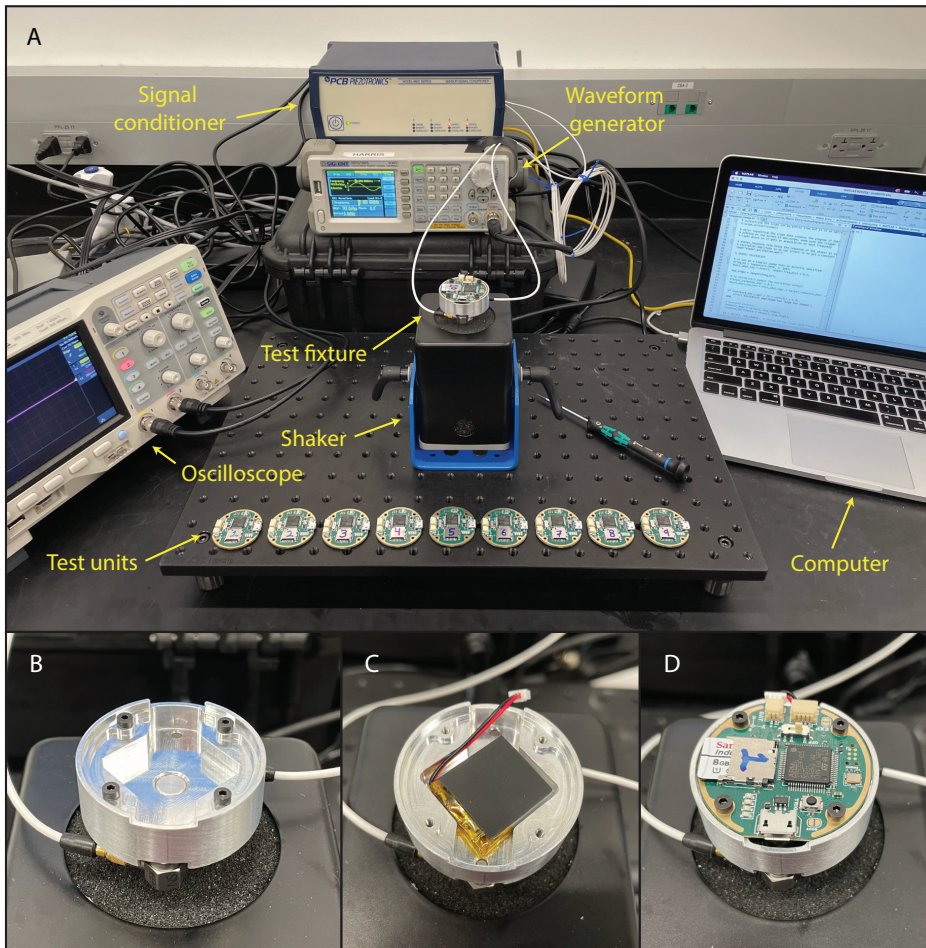


Figure 3: (A) Shaker setup used to measure the frequency response of the 10 nominally equivalent IMpack test units. (B) Closeup of the machined aluminum test fixture attached to the shaker mounting point with the uniaxial reference accelerometers installed. (C) The battery that powers the IMpack is inserted into the pocket in the test fixture and an adhesive rubber pad is applied between the battery and the IMpack to mitigate vibrations of the PCB. (D) The IMpack is installed atop the battery using four M2 cap screws.

ital oscilloscope (Siglent SDS1204X-E). The excitation signal for the shaker is produced by a waveform generator (Siglent SDG1025). The testing setup is coordinated by a host computer that controls the waveform generator and oscilloscope through their Standard Commands for Programmable Instruments (SCPI) interfaces over USB serial connections. The frequency response of each of ten nominally equivalent IMpack test units is evaluated using the setup. At each frequency step, the host computer first commands the appropriate amplitude and frequency from the waveform generator via a MATLAB script. Then it sets the scale of the oscilloscope appropriately in order to capture several periods of vibration. Finally the acceleration signals from the oscilloscope are streamed to the computer to be stored for later processing. The frequency sweep is performed from 20 Hz to 10 kHz in 100 steps with logarithmic increments. The shaker excitation voltage at each frequency step is chosen such that the acceleration amplitude as measured by the average of the two uniaxial accelerometers is 5.0 ± 0.1 g. When assembling the IMpack fixture, the battery that powers the IMpack is inserted into the pocket in the aluminum part and an adhesive rubber pad (McMaster-Carr 1374N13) is applied between the battery and the IMpack to mitigate vibrations of the PCB as shown in figure 3(C). Finally the IMpack unit to be tested is fastened onto the fixture with four M2 cap screws as shown in figure 3(D). The IMpack continuously records data to the SD card during the frequency sweep.

Figure 4 illustrates the results of the IMpack frequency response testing. The amplitude of an acceleration signal $|a|$ at a given frequency step is computed using the root-mean-squared (RMS) method (Horowitz et al. 2015) as

$$|a| = \sqrt{\frac{2}{n} \sum_i a_i^2} \quad (1)$$

where a_i is a particular acceleration sample in the signal with n total samples. We typically capture 15 oscillation cycles at each frequency step in our testing and the system is allowed ample settling time after each frequency change before capturing data. When using the RMS amplitude estimation method on the real signals, we first remove the mean value of the signal due to gravity and then set the bounds of the summation at zero crossings to increase accuracy. This method will accurately capture the amplitude of a purely sinusoidal signal but some error in the amplitude estimation is present in practice, especially near the system resonant modes. In particular, large amplitude oscillations or bending modes of vibration at or near the resonant modes introduce nonlinearity into the system that manifests as harmonic distortion of the signal. The RMS method captures this additional frequency content in the amplitude estimation whereas a method based on the Fourier transform would only capture the amplitude of the signal content at the target excitation frequency. Nevertheless, we select the RMS method because it has the advantage of providing an estimate of the amplitude even when the excitation frequency exceeds the sensor's Nyquist frequency, thereby revealing the analog anti-aliasing capability of the sensor chip which is important to characterize when sampling high-frequency acceleration signals. Figures 4(A-C) show the frequency response of the three IMU chips on the IMpack as compared to the reference uniaxial accelerometer. The cor-

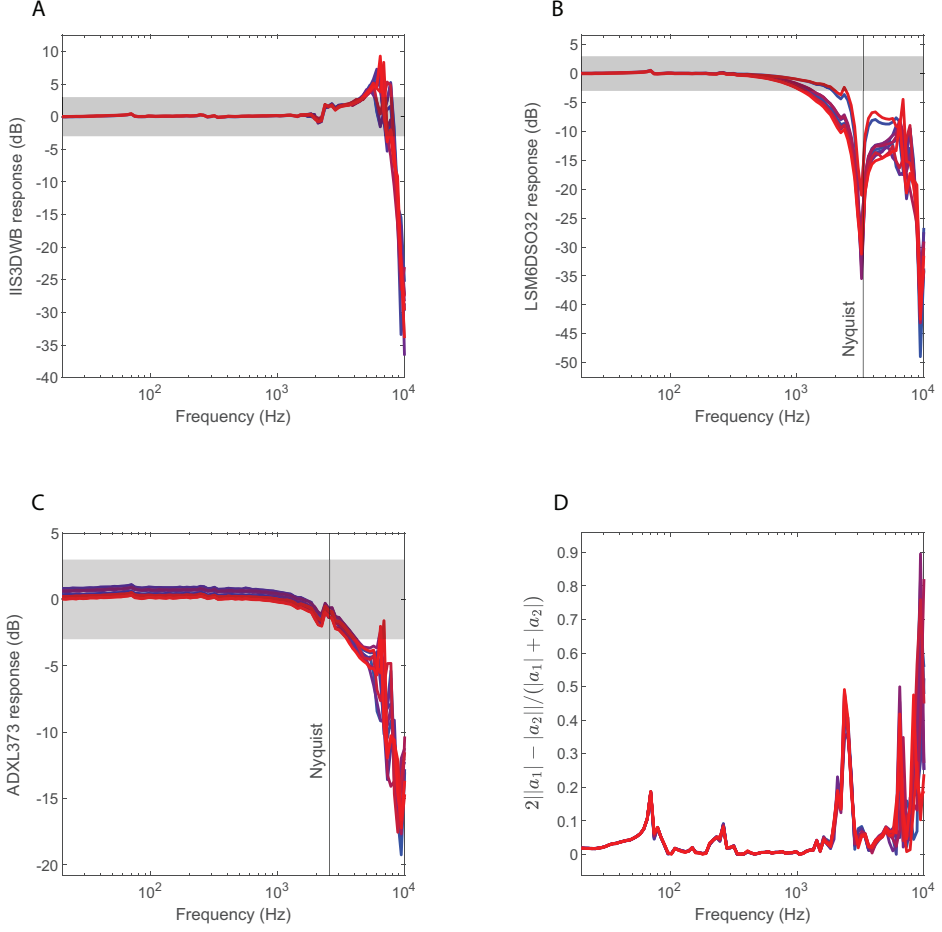


Figure 4: (A) Frequency response of the IMPack IIS3DWB accelerometer chip compared to the uniaxial reference accelerometer (PCB Piezotronics 352C65). The shaded region indicates the ± 3 dB band corresponding to the commonly used half power bandwidth criterion. The sampling rate of this chip is 26.6 kHz so the Nyquist frequency is not shown. Each plot features the results from each of the 10 IMPack test units. (B) Frequency response of the IMPack LSM6DSO32 accelerometer chip compared to the uniaxial reference accelerometer. The Nyquist frequency is shown as a vertical line. (C) Frequency response of the IMPack ADXL373 accelerometer chip compared to the uniaxial reference accelerometer. The signal to noise ratio is worse for this ± 400 g IMU chip since our shaker is incapable of producing such large accelerations, leading to more variation in the results. (D) The test fixture features two uniaxial reference accelerometers fastened to opposite sides. This plot illustrates the magnitude of the difference between the two channels as a function of the shaker excitation frequency. Large differences between the two channels indicate a structural resonance in the shaker which features tilting or other off-axis motion instead of the desired purely axial motion. The amplitude of the excitation voltage is chosen to target a 5 g axial acceleration amplitude of the shaker across the frequency test range.

ner frequency of each chip's digital low pass filter is set as high as possible so that the filter has minimum influence on the results. In the frequency response plots, only the rear uniaxial accelerometer is used in the comparison since it is most proximal to the IMU chips on the IMpack and thus is less susceptible to measurement discrepancy due to erroneous off-axis motion of the shaker. Each of the plots contains the result from each of the ten IMpack test units, demonstrating that there is minimal variation with the population manufactured. The shaded areas indicate the ± 3 dB region which may be used as a criterion for the IMU chip's bandwidth. All of the chips' bandwidths exceed 1 kHz with minimal ripple in the pass band. The bandwidth of the IIS3DWB chip is closer to 6 kHz at which point the frequency response enters an amplification region. There is greater variation in the results for the ADXL373 chip because the signal to noise ratio is unfavorable for this high-g sensor at the low acceleration values tested. Figures 4(B) and (C) additionally show the Nyquist frequency (half of the sampling frequency) of the IMU chip (the IIS3DWB Nyquist frequency exceeds 10 kHz) which can be used to evaluate the performance of the analog anti-aliasing performed by the chip. Any frequency content that exists beyond the Nyquist is due to non-physical aliased components of the signal, suggesting that the LSM6DSO32 chip performs more effective anti-aliasing than the ADXL373 chip. Figure 4(D) shows the normalized magnitude of the amplitude difference between the two uniaxial reference accelerometer signals a_1 and a_2 as a function of frequency during each of the ten frequency sweep trials. A value on the ordinate of zero suggests that the motion of the test fixture is purely vertical, as intended. However, deviations arise at the resonant frequencies of the system where off-axis motion of the shaker occurs. These resonant modes correlate with the small blips observed in the pass band of the IMU chip frequency response plots.

General testing

The IMpack battery charge rate is 100 mA, meaning that the 150 mAh battery used in our testing charges in approximately 1.5 hrs. The average current consumption is 55 mA when idle, 65 mA when recording data, and 85 mA when formatting the data after a recording so recording times exceeding 2 hrs are possible on a single charge. Larger batteries may be substituted for longer recording times, or the device can be powered over USB indefinitely. Simple test scripts confirm the basic functionality of the USB and I2C ports for data transfer. An important factor to consider is the potential for data loss during a recording. The maximum write latency of the SD card used (SanDisk Industrial 8 GB) is specified as 250 ms, meaning that the RAM double buffer would need to contain 500 ms worth of data to guarantee no data loss. With the very fast sampling rates used and limited MCU RAM, this is not feasible. However, the actual latency of SD cards tends to be far smaller than the data sheet upper bound. In our testing with the industrial micro SD card the actual write latency is small enough in practice that data loss is exceedingly rare. In the IMpack data file, each data point contains a time stamp captured from a hardware timer with one microsecond period. Thus the interval between successive data points in the file can be calculated and compared with the target sampling frequency to check each individual file for data loss depending on the user's SD card.

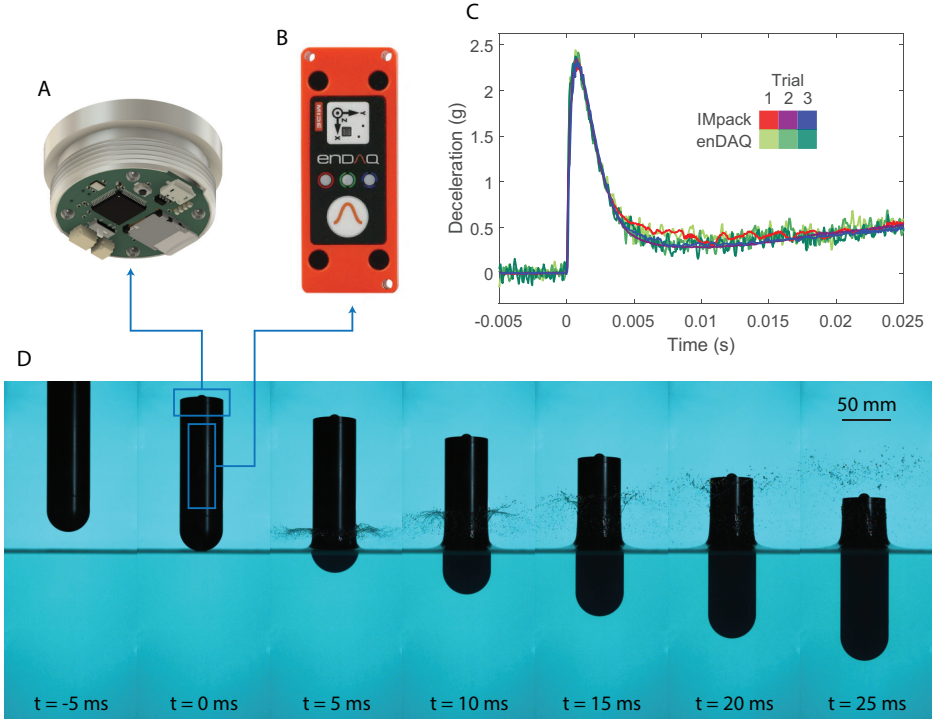


Figure 5: (A) The IMpack is mounted in an aluminum fixture that threads into the end of a slender axisymmetric anodized aluminum impactor with hemispherical nose. (B) A commercial data logging IMU (enDAQ S4-R100D40) is mounted in the central body of the impactor. (C) The impactor enters the water at 4 m/s and its deceleration is recorded using the onboard IMpack and commercial enDAQ accelerometer simultaneously. The hemispherical nose has radius 22.23 mm and the total mass of the impactor is 0.568 kg. The enDAQ samples at 20 kHz with a piezoelectric sensing element with ± 100 g range. The IMpack samples at 26.6 kHz using the IIS3DWB chip with ± 16 g range. Simultaneous recordings from both accelerometers during three independent drop trials are shown. (D) Time series photographs of the impactor with the onboard IMUs entering the water.

(3) Application

Water impact experiments

We demonstrate an application for the IMpack in which it is used to measure the hydrodynamic force on a rigid body as it lands on the water's surface, with the results shown in figure 5. Water entry is an active area of engineering research due to its myriad applications to aerospace and naval vehicles as well as biological divers (Abbate 2013, Seddon & Moatamed 2006, Li et al. 2025, Pandey et al. 2022). The impact force on a spherical object is well known from both classic mathematical solutions (Shiffman & Spencer 1945) as well as experiments (Moghisi & Squire 1981), motivating the use of an impactor with a hemispherical nose in the IMU validation experiments presented here. As shown in figure 5(D), the axisymmetric impactor is elongated to accommodate mounting both the IMpack as well as an industry standard commercial data logging

IMU (enDAQ S4-R100D40). The impactor is machined from ASTM 6061-T6 aluminum and is anodized black, and features a nose radius and overall radius of 22.23 mm, length of 220 mm, and mass of 0.568 kg (fully assembled). We fabricated a threaded end cap to hold the IMpack as shown in figure 5(A) which attaches to the trailing end of the impactor with a water-tight seal. The commercial IMU shown in figure 5(B) is rigidly affixed within the main body of the impactor using a threaded clamping ring. We drop the impactor with normal incidence into a large water bath from a height such that the speed of the impactor when it first contacts the water surface is 4 m/s and record the acceleration using both the IMpack and the commercial IMU simultaneously. We film the impact event with a high-speed camera that produces the time series photographs in figure 5(D). The corresponding acceleration traces recorded in each of three experimental trials are shown in figure 5(C). The impactor experiences a sharp impulsive deceleration at first contact which corresponds to the rapidly developing hydrodynamic loading, lasting less than 5 ms for the parameters of these experiments. The fast time scales of loading during water entry motivate the need for very high bandwidth IMUs like the IMpack. In these experiments, the enDAQ IMU samples at 20 kHz using a piezoelectric sensing element with ± 100 g range. The manufacturer's listed bandwidth is 2 kHz though a more conservative metric is used than the typical half power criterion. The IMpack samples at 26.6 kHz using the IIS3DWB chip with ± 16 g range, with the chip's digital low pass filter configured to provide a -3 dB bandwidth of 1.3 kHz. In each case the mean acceleration reading during free fall is subtracted from the measurements so that only the contribution from the hydrodynamic loading is shown (the DC component of enDAQ reading drifts with temperature). The IMpack measurement agrees excellently with the reference IMU and, for the case tested, features lower noise since the measurement range is better suited to the magnitude of the acceleration experienced by the impactor. The comparison provides confidence that the IMpack can be used to take accurate measurements of the deceleration during water entry experiments in a more compact package with significantly lower cost. The absence of drift in the DC component of the acceleration signal compares favorably against the enDAQ IMU's piezoelectronic accelerometer channel. Additionally, the IMpack produces a plain text CSV data file which can be directly analyzed whereas the enDAQ IMU's binary data file format requires post processing.

(4) Build Details

Availability of materials and methods

Most of the components chosen for the IMpack PCB are generic and readily available from a number of manufacturers. The STM32F405 micro-controller cannot be easily substituted and is only available from one manufacturer but is widely available as it is part of ST's foundation line of high performance microcontrollers. Similarly the Hirose DM3D-SF SD card holder is specifically required due to its compact size but is also widely available. The battery charge manager chip MCP73871 is another manufacturer specific chip that is readily available. The specialty IMU chips, namely the high-g ADXL373 and high-bandwidth IIS3DWB, can be more difficult to find and make up the

majority of the component cost of the IMpack. These chips can be omitted altogether without otherwise compromising the functionality and the IMpack can be constructed with only the readily available LSM6DSx chip as a low-cost fallback option. Additionally, the IMU chip manufacturers offer some pin-for-pin compatible substitutions with similar performance, such as Analog Devices' ADXL372 in place of the ADXL373 (though we caution that the ADXL372 produces erroneous harmonics in its output as documented in the chip's errata). ST's high-bandwidth IIS3DWB can be directly replaced with many chips from the LSM6DSx line. Of course substituting an IMU chip will require minor modifications to the firmware in order to work correctly. The IMpack will work with any single cell lithium polymer battery that can support at least 100 mA charge rate. It uses a JST-SH battery connector to save space but the most commonly available batteries have a JST-XH connector. If a battery with the proper connector cannot be purchased, the connector can be re-crimped or a pigtail with the correct connector can be soldered. Although not part of the device itself, the IMpack will require a mounting fixture in most applications. Example designs for the mounting fixture can be found in the associated documentation. The fixture can be 3D printed if tight control over the resonant modes is not required (*e.g.* in educational use or measurement of small accelerations at low frequencies) which is a widely available process. The reported results use machined aluminum housings which require a more specialized process, but one that is becoming increasingly accessible through advances in desktop machining centers.

Ease of build

The IMpack PCB uses a four layer stackup with double sided assembly which likely precludes its fabrication using DIY techniques but is necessary to preserve the overall compact footprint of the device. However, attention is paid to the ease of manufacture of the design so that it can be affordably produced by commercial PCB prototype manufacturers. Most of the passive components in the design are grouped into common values in order to consolidate the bill of materials. The minimum trace width is 0.15 mm (5.9 mil) and the minimum via size is 0.65 mm (25.6 mil) with a 0.25 mm (9.8 mil) hole which are well within the manufacturing capabilities of most board manufacturers without increasing the manufacturing cost. Adequate space is provided between PCB components to facilitate automated assembly and around the mounting holes to avoid mechanical interferences. Additionally, component packages with exposed leads are chosen wherever possible to aid potential hand soldering or voltage measurements while debugging the design. The smallest component package size is 0402 which is within the capability of most PCB prototype manufacturers' economic assembly options. A boot mode jumper is provided to recover the micro-controller in case of a failed programming. Connector polarity indicators, measurement axis directions, and other silkscreen markings are provided for ease of use.

Operating software and peripherals

The IMpack firmware is written in C and developed using the toolchain provided with STM32CubeIDE version 1.16.0. The compiled firmware uses only 60 kB of

the available 1 MB of code space. During execution, 116 kB of the available 128 kB of general purpose RAM is utilized. However, the 64 kB core coupled RAM region is unused and available for future extensions of the firmware. During operation, the device is configured using a plain text file on the SD card which can be set up in any text editor. The acquired IMU data is typically encoded in a plain text CSV file which can be further processed with Excel, MATLAB, Python, *etc.* In cases with high sampling rate and long measurement times, using the onboard micro-controller to convert the binary data to plain text can take a prohibitive amount of time so the plain text formatting can be disabled in the settings. In this case the binary data file must be parsed with user software. Examples are provided in Python and MATLAB in the associated documentation.

Dependencies

The software for the IMpack is written with minimum dependencies. The only software dependency is the microcontroller manufacturer ST's Hardware Abstraction Layer library provided in the STM32Cube FW_F4 V1.28.1 firmware package.

Documentation and files location

Archive for hardware and software documentation and build files.

Name: IMpack

Persistent identifier: <https://github.com/harrislab-brown/IMpack>

License: CC BY-SA 4.0 Creative Commons

Publisher: Daniel M. Harris

Date published: 03/12/2025

This archive contains the modifiable build files and software at the time of publication. The current version is available in a GitHub repository at <https://github.com/harrislab-brown/IMpack>.

(5) Discussion

Conclusions

We have presented the design and validation of the IMpack, a low-cost, compact, and high-performance single board data-logging inertial measurement unit for research applications. The IMpack includes an array of three MEMS accelerometer chips with different strengths so that the most appropriate sensor can be used for the requirements of a given measurement. The IMpack records three axes of acceleration and angular rotation rate to a micro SD card with sampling rates up to ± 26.6 kHz, acceleration measurement range up to ± 400 g, and angular rate measurement range up to ± 2000 deg/s. It is powered from a single cell lithium polymer battery and features charging circuitry allowing the device to be charged easily over its micro USB port. The measurement parameters are highly configurable using a plain text file on the SD card. The

diameter of the device is 38 mm, the overall thickness including the battery is 13 mm, and the overall mass including the battery is 9 grams. In the limited quantities that we manufactured, the cost per board was well below 100 USD. We characterized a population of ten IMpack units by measuring the frequency response of each channel up to 10 kHz in a shaker setup, comparing against a calibration piezoelectronic uniaxial accelerometer. Additionally, we demonstrated a research application for the IMpack in which it is used to measure the force of impact as a structure lands on the water surface, comparing the measurement directly against an industry standard commercial data-logging IMU costing over an order of magnitude more with excellent agreement. With the low-cost IMpack design, we demonstrate how the industry trend of ever better and cheaper MEMS devices and microcontrollers can be successfully leveraged to create useful and accessible research devices. The IMpack will make highly resolved acceleration measurements more accessible in a range of engineering research areas including experimental modal analysis, impact dynamics and automotive design, as well as in educational settings.

Future Work

Several additional functionalities could be achieved with the IMpack through extensions of the firmware. For instance, the I2C/GPIO expansion port would enable synchronization of several IMpack devices in order to measure vibration of a structure at multiple locations. Such a setup could be used to experimentally deduce the vibrational mode shapes of the structure. Additionally, although the current implementation only uses the USB port for charging, the MCU contains an internal USB full speed physical layer so the port could be used for communication with a host computer as well. This may be beneficial in educational scenarios where data streamed from the IMpack could be interactively plotted in real time with a host application and logged for later analysis. Furthermore, additional testing and software consideration for very long time recordings, such as those performed in building monitoring applications, would be a useful future direction since the present version was primarily designed for impact experiments with very short time scales.

The power circuitry of the IMpack presents another opportunity for refinement since the current design expects the battery to have its own shutoff circuitry to prevent damage from excessive discharge. Most of the commercially available lithium polymer battery cells do contain this protection circuitry already, but adding it to the IMpack PCB would make the design compatible with an even wider array of batteries.

Another avenue for improvement would be to extend the available RAM in order to guarantee no data is lost while logging due to the SD card write latency. One option would be to add an external synchronous dynamic random access memory (SDRAM) chip and integrate it with the MCU's flexible memory controller (FMC) hardware, but board space is limited. Another route would be to utilize the new STM32H563 microcontroller line which features far more RAM than the current microcontroller as well as higher core clock speed in the same footprint, but availability is currently limited and costs are higher. Finally, established lines of higher performance microcontrollers with more RAM are available in highly compact ball grid array (BGA) packages, but hand soldering would then

be impossible and the PCB would require more layers to route properly, increasing costs. Although data loss cannot be guaranteed to not occur with the present design, in practice the SD card write latency is typically far lower than the worst case values presented by the data sheet and data loss (which is easily detectable using the time stamps in the data file) has not been an issue in our experience with using the device.

The addition of a magnetometer would likely be feasible due to their compact size and would permit absolute orientation measurement, facilitating estimation techniques such as position dead reckoning.

Finally, there is a need for MEMS accelerometer chips with both high bandwidth and a large measurement range. The current high-bandwidth IIS3DWB accelerometer chip used on the IMPack features a maximum acceleration measurement of ± 16 g which is sometimes exceeded in our impact experiments, requiring us to fall back to the lower-bandwidth measurements from the other IMU chips. Chips with the same bandwidth but higher measurement range are not available. In this regard, piezoelectric accelerometers are superior but they tend to have lower availability and higher costs, and require the PCB designer to implement bespoke analog-to-digital conversion circuitry, motivating our choice of MEMS sensors.

Paper author contributions

JTA designed the hardware, coordinated the manufacturing process, wrote the software, and performed the testing. DMH advised and oversaw the project. JTA and DMH designed the testing, wrote the manuscript, and prepared the file repository.

Acknowledgments

We thank Eli Silver for early discussions regarding the design concept of the device and IMU chip selection. We thank Ashley Kraekel and Tristan Keyser-Parker for their feedback on the IMPack user experience while they utilize the device to perform water entry experiments. We thank Tristan Keyser-Parker for his help with machining the water impactor IMPack mounting fixture. The authors also thank Jesse Belden (Naval Undersea Warfare Center, Newport, RI) for guidance and feedback throughout the project.

Funding statement

We gratefully acknowledge funding from the Office of Naval Research (ONR N00014-21-1-2816) and the NASA-Rhode Island Space Grant Consortium.

Competing interests

The authors declare that they have no competing interests.

Copyright notice

©2025 The Author(s). This is an open-access article distributed under the terms of the Creative Commons Attribution 4.0 International License (CC-BY 4.0), which permits unrestricted use, distribution, and reproduction in any medium, provided the original author and source are credited. See <http://creativecommons.org/licenses/by/4.0/>.

References

- Abrate, S. (2013), 'Hull Slamming', *Applied Mechanics Reviews* **64**(6). 060803.
URL: <https://doi.org/10.1115/1.4023571>
- Ahmad, N., Ghazilla, R. A. R., Khairi, N. M. & Kasi, V. (2013), 'Reviews on various inertial measurement unit (imu) sensor applications', *International Journal of Signal Processing Systems* **1**(2), 256–262.
- Antolik, J. T., Belden, J. L., Speirs, N. B. & Harris, D. M. (2023), 'Slamming forces during water entry of a simple harmonic oscillator', *Journal of Fluid Mechanics* **974**, A23.
- Debenedetti, F. & Jung, S. (2024), 'Effect of feathers on drag in plunge-diving birds', *Annals of the New York Academy of Sciences* **1537**(1), 74–81.
- Friman, S. I., Elowe, C. R., Hao, S., Mendez, L., Ayala, R., Brown, I., Hagood, C., Hedlund, Y., Jackson, D., Killi, J. et al. (2024), 'It pays to follow the leader: metabolic cost of flight is lower for trailing birds in small groups', *Proceedings of the National Academy of Sciences* **121**(26), e2319971121.
- Hanly, S. (2019), 'Rating my top 11 vibration data loggers', <https://blog.endaq.com/review-of-top-11-vibration-data-logger-products>. Accessed: 3-7-2025.
- Harris, D. M. & Bush, J. W. (2015), 'Generating uniaxial vibration with an electrodynamic shaker and external air bearing', *Journal of Sound and Vibration* **334**, 255–269.
- Horowitz, P., Hill, W. & Robinson, I. (2015), *The art of electronics*, Vol. 3, Cambridge university press Cambridge.
- Li, S., An, K., Huang, W., Li, S. & Liu, S. (2025), 'Research progress of high-speed water entry for trans-media vehicles: State-of-the-art review', *International Communications in Heat and Mass Transfer* **161**, 108453.
- Moghisi, M. & Squire, P. (1981), 'An experimental investigation of the initial force of impact on a sphere striking a liquid surface', *Journal of Fluid Mechanics* **108**, 133–146.
- Pandey, A., Yuk, J., Chang, B., Fish, F. E. & Jung, S. (2022), 'Slamming dynamics of diving and its implications for diving-related injuries', *Science Advances* **8**(30), eab05888.
- Rabbi, R., Speirs, N. B., Kiyama, A., Belden, J. & Truscott, T. T. (2021), 'Impact force reduction by consecutive water entry of spheres', *Journal of Fluid Mechanics* **915**, A55.
- Seddon, C. & Moatamed, M. (2006), 'Review of water entry with applications to aerospace structures', *International Journal of Impact Engineering* **32**(7), 1045–1067.
- Shiffman, M. & Spencer, D. C. (1945), The force of impact on a sphere striking a water surface: second approximation, Technical Report AMG-NYU-133, New York University, Courant Institute of Mathematical Sciences.